ACS APPLIED MATERIALS & INTERFACES

Research Article

www.acsami.org

Solution-Processed Ag Nanowires + PEDOT:PSS Hybrid Electrode for Cu(In,Ga)Se_2 Thin-Film Solar Cells

Donghyeop Shin,[†,‡] Taegeon Kim,[§,‡] Byung Tae Ahn,*[,†] and Seung Min Han*[,§]

[†]Department of Materials Science and Engineering and [§]Graduate School of Energy Environment Water and Sustainability, Korea Advanced Institute of Science and Technology, 291 Daehak-ro, Yuseong-gu, Daejeon 305-701, Republic of Korea

ABSTRACT: To reduce the cost of the Cu(In,Ga)Se_2 (CIGS) solar cells while maximizing the efficiency, we report the use of an Ag nanowires (NWs) + poly(3,4-ethylenedioxythiophene):poly(styrenesulfonate) (PEDOT:PSS) hybrid transparent electrode, which was deposited using all-solution-processed, low-cost, scalable methods. This is the first demonstration of an Ag NWs + PEDOT:PSS transparent electrode applied to CIGS solar cells. The spin-coated 10-nm-thick PEDOT:PSS conducting polymer layer in our hybrid electrode functioned as a filler of empty space of an electrostatically sprayed Ag NW network. Coating of PEDOT:PSS on the Ag NW network resulted in an increase in the short-circuit current from 15.4 to 26.5 mA/cm^2, but the open-circuit voltage and shunt resistance still needed to be improved. The limited open-circuit voltage was found to be due to interfacial recombination that is due to the ineffective hole-blocking ability of the CdS film. To suppress the interfacial recombination between Ag NWs and the CdS film, a Zn(S,O,OH) film was introduced as a hole-blocking layer between the CdS film and Ag NW network. The open-circuit voltage of the cell sharply improved from 0.35 to 0.6 V, which resulted in the best cell efficiency of 11.6%.

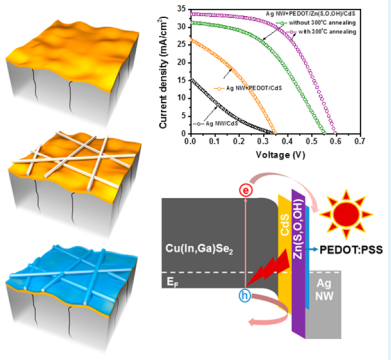

KEYWORDS: *Ag nanowire, solution process, Ag nanowires + PEDOT:PSS hybrid transparent electrode, Zn(S,O,OH), hole-blocking layer, Cu(In,Ga)Se_2 solar cell*

1. INTRODUCTION

Solar cells that convert sunlight directly into electricity have potential as a major source in power generation. Presently, the crystalline Si solar cells dominate the solar cell market share by more than 80%; however, the material cost of the cell occupies over 50% of the total manufacturing cost, which makes this technology less competitive in comparison to the conventional power generation by fossil fuels.[1] One method to reduce the material cost is to fabricate solar cells in thin films instead of using a thick Si wafer. Thin-film Si solar cells, however, suffered from low efficiency, and thus different material options that can overcome the low efficiency were researched. Cu(In,Ga)Se_2 (CIGS) and CdTe thin-film solar cells are currently being developed, but the CIGS solar cell is considered as the most promising technology because of a high efficiency in the range of >20%, which is significantly surpasses that of the thin-film Si solar cell.[2,3] However, the manufacturing cost of CIGS thin-film solar cells still remains a challenge in order to make a cost-effective solution to today's energy consumption needs.

Many attempts were made to reduce the manufacturing cost of CIGS solar cells by lowering of both the processing and materials costs. First, the preparation of the absorber was successfully demonstrated using nonvacuum processes, such as the solution-based method where the solution for the absorber layer is deposited by screen-printing or spin-coating methods.[4−6] Recently, these nonvacuum-processed CIGS solar cells showed up to 16% efficiency, but such high efficiency is unfortunately constrained to laboratory-scale or small areas because of poor film uniformity and reproducibility. Another way to reduce the manufacturing cost of CIGS solar cells is to replace the rare elements In and Ga with earth-abundant elements such as Zn and Sn, but it is also difficult to deposit a high-quality Cu_2ZnSnS_4 or $Cu_2ZnSnSe_4$ because of the easy formation of the binary compounds ZnSe, ZnS, $MoSe_2$, and MoS_2 and the highly volatile Sn element.[7−9] Studies for lowering the processing and materials costs further are being actively researched currently.

Although there were concentrated efforts in the development of solution processing of the absorber layer, the development of the solution-processed transparent electrode to replace the ZnO or ITO in CIGS solar cells was not extensively studied. It is well-known that the metal nanowire (NW) network is a promising flexible transparent electrode material with excellent optical and electrical properties with a cost-effective processing method, where the NWs are synthesized in solution and simply spray- or spin-coated on a substrate of desired choice.[10,11] The Ag NW network as a transparent electrode was demonstrated many times for the case of flexible display panels or flexible organic solar cells,[12−14] but limited studies were conducted for the case of CIGS solar cells. For cost-effective CIGS solar cells, an Ag NW composite with indium−tin oxide (ITO) nanoparticles (NPs) was first adapted to use as an alternative

Received: April 6, 2015
Accepted: May 27, 2015
Published: May 27, 2015

DOI: 10.1021/acsami.5b02989
ACS Appl. Mater. Interfaces 2015, 7, 13557−13563

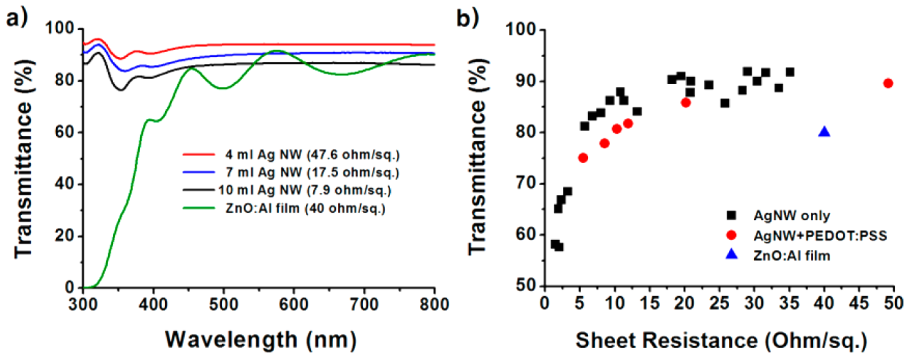

Figure 1. (a) Transmittance of the ZnO:Al film and the Ag NW network with various densities: 4, 7, and 10 mL. (b) Transmittance (average of 400−800 nm) versus sheet resistance comparison between the Ag NW electrode and ZnO:Al film on a glass substrate.

transparent electrode.[15] The cell with the Ag NWs + ITO NPs composite electrode achieved an efficiency of above 10%. Additionally, there was an Ag NWs composite electrode with sol−gel-processed ZnO instead of ITO NPs.[16] However, the Ag NWs composite electrode still uses the conducting oxide materials (ITO or ZnO) of the conventional transparent electrode. Most recently, a solution-processed graphene oxide (GO)-welded Ag NWs transparent electrode was developed.[17] The GO nanosheet was employed as an adhesive material to enhance the series resistance of organic−Si hybrid solar cells.

In this study, instead of the conducting oxide, a poly(3,4-ethylenedioxythiophene):poly(styrenesulfonate) (PEDOT:PSS) conducting polymer was used to help the Ag NW network to effectively collect generated charges and improve adhesion to the surface. Most of all, PEDOT:PSS can completely fill in the vacant spacing of the Ag NW network. Thus, an Ag NWs + PEDOT:PSS hybrid electrode was demonstrated for the first time as a transparent electrode for CIGS solar cells. For high efficiency, it is very important to effectively separate generated charges without an interfacial recombination at the junction. Thus, a hole-blocking layer to prevent the interfacial recombination was introduced between the CIGS absorber and the Ag NWs + PEDOT:PSS electrode. The solution-processed, highly conductive, and transparent Ag NWs + PEDOT:PSS hybrid electrode appears to be a good solution for reducing the manufacturing cost of CIGS thin-film solar cells. Furthermore, it can be realized with flexible solar cells.

2. EXPERIMENTAL SECTION

2.1. Chemicals and Materials. Poly(vinylpyrrolidone) (PVP; $M_w \approx$ 55000, powder), dimethyl sulfoxide (DMSO; 99.9%), cadmium sulfate ($CdSO_4$; 99.99%), zinc sulfate ($ZnSO_4$; 99.9%), and thiourea ($(NH_2)_2CS$; 99.0%) were purchased from Sigma-Aldrich. PEDOT:PSS (Clevios PH 1000) was purchased from Heraeus Precious Metals GmbH & Co. KG. Silver nitrate ($AgNO_3$; 99.0%), sodium chloride (NaCl; 99.5%), potassium bromide (KBr; 99.0%), ethylene glycol (EG; 99.0%), and ammonia solution (NH_4OH; 28−30%) were purchased from a common commercial supplier. All chemicals were used without further purification.

2.2. Synthesis of the Ag NW Solution and Its Application to the Composite Electrode. Ag NWs were synthesized by a solution-processing method known as the polyol reduction method[18] with modifications. EG, which was a solvent of the synthesis method, played a role as the reductant for reducing Ag^+ ions to form the Ag^0 NP seeds. Dissolved PVP induced anisotropic growth of the NW along the [110] directions by preferentially binding to the (111) surfaces of the Ag NPs. Ag NWs with an enhanced aspect ratio were obtained by adding KBr as well as using NaCl instead of AgCl to improve the anisotropic growth of the NWs.[19] The details of the Ag NW synthesis were described in our previous work.[20] The density of the Ag NWs dispersed in methanol was measured by drying and weighing a measured volume of a well-dispersed Ag NW solution.

The Ag NWs dispersion in methanol with an optimized concentration of 0.5 mg/mL was deposited on a CIGS solar cell using a commercially available electrostatic spray system from NanoNC, Inc. The syringe was loaded with the NW solution and held at 15 kV, while the PC substrate was held at the ground at a distance of 3.6 cm away from the tip. The injection rate for the solution was 20 mL/h, and the density of the NW deposition was controlled by the volume of the sprayed solution.

After deposition of the Ag NW electrode, a rapid thermal annealing (RTA) was performed to reduce the junction resistance or to lower the sheet resistance of the NW network. Then, NH_4OH-added PEDOT:PSS with 5 wt % DMSO (pH 7−9) was spin-coated on the Ag NW electrode to solve the problem of the poor contact between the CdS layer with a rough surface and the Ag NWs. The difficulty of carrier transport from the surface of the CdS layer to the Ag NWs due to the low surface contact area between the Ag NWs and the CdS layer was also solved by coating the PEDOT:PSS layer.

2.3. Fabrication of CIGS Solar Cells Employing the Ag NWs + PEDOT:PSS Electrode. CIGS absorber layers were deposited on Mo-coated glass substrates using a coevaporation system.[21,22] The composition of the CIGS film was adjusted to be $Cu(In_{0.7}Ga_{0.3})Se_2$. A 50-nm-thick CdS buffer layer was grown on the CIGS absorber layer using the chemical bath deposition (CBD) process from an alkaline aqueous solution of $CdSO_4$, $(NH_2)_2CS$, and NH_4OH.[23] To prevent interfacial recombination between CdS and Ag NWs, a 70-nm-thick Zn(S,O,OH) layer was grown on a CdS buffer layer using the CBD process. For growth of the Zn(S,O,OH) film, $ZnSO_4$, $(NH_2)_2CS$, and NH_4OH were used. After the Zn(S,O,OH)/CdS/CIGS film growth, the samples were annealed in ambient air using a RTA process. The RTA process has the advantages of a lower thermal budget and precise processing time to minimize the intermixing at the Zn(S,O,OH)/CdS/CIGS interface. The samples were annealed at 300 °C. Then, the samples were left to cool naturally. To complete the CIGS solar cells, the Ag NWs + PEDOT:PSS electrode was applied on the Zn(S,O,OH)/CdS/CIGS film.

2.4. Thin-Film and Device Characterization. The optical properties of the samples were investigated via UV−visible spectroscopy using a Shimadzu UV 3600 spectrometer. The morphology and thickness of the films were investigated via field-emission scanning electron microscopy (SEM) using a Hitachi S-4800 microscope without a conductor coating. To determine the valence-band offset (VBO) at the Zn(S,O,OH)/CdS/CIGS interface, valence-band maximum (VBM) values of three layers such as a bare CIGS film, CdS on CIGS, and Zn(S,O,OH) on CdS/CIGS were measured via ultraviolet photoelectron spectroscopy (UPS) using a Thermo Scientific Sigma probe.[24,25] The current density−voltage (J−V) characteristics were measured at 25 °C under illumination using a Spectra Physics Oriel 300 W Solar Simulator with an AM 1.5G filter. A calibrated Si cell was used as a reference for J−V.

DOI: 10.1021/acsami.5b02989
ACS Appl. Mater. Interfaces 2015, 7, 13557−13563

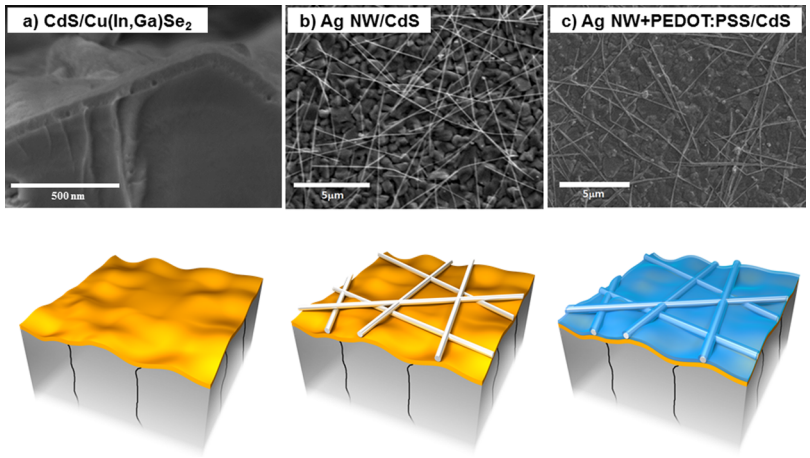

Figure 2. Cross-sectional SEM images of (a) CdS/CIGS, (b) Ag NWs/CdS/CIGS, and (c) Ag NWs + PEDOT:PSS/CdS/CIGS films.

3. RESULTS AND DISCUSSION

To develop a novel transparent electrode using Ag NWs, the optical and electrical properties of the Ag NW network were first characterized. The transmittances of the Ag NW network with various densities as well as the ZnO:Al film are shown in Figure 1 for comparison. Figure 1b shows a trade-off between the transmittance and electrical conductivity of the Ag NW transparent electrode because the usage of a higher density of NWs can result in enhancement in the conductivity while the corresponding light shadowing effect can lower the overall transmittance. The sheet resistance of the Ag NW network with a spray volume of 4 mL is similar to that of the conventional ZnO:Al film (350 nm). It should be noted that the Ag NW network has an advantage over the ZnO:Al film in that ZnO:Al has poor transmittance at the short-wavelength region (300–500 nm) while the Ag NW network has excellent transmittance over the wavelength range 300–800 nm. Thus, a Ag NW transparent electrode prepared with 7 mL of spray volume was chosen in order to optimize the efficiency of the CIGS solar cell. The chosen density of the Ag NWs showed higher electrical conductivity than the ZnO:Al film on the same optical transmittance condition.

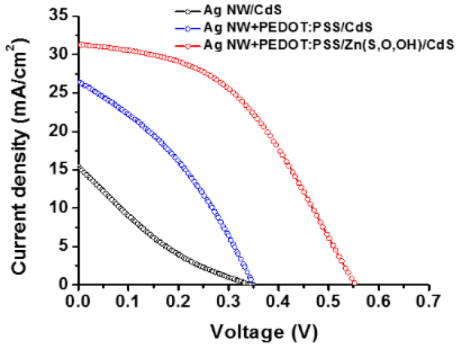

	V_{OC} (V)	J_{SC} (mA/cm²)	FF	Effi. (%)	R_S (Ωcm²)	R_{Sh} (Ωcm²)
Ag NW /CdS	0.34	15.4	0.18	0.9	13.9	16.4
Ag NW + PEDOT:PSS /CdS	0.35	26.5	0.35	3.2	4.3	26.1
Ag NW + PEDOT:PSS /Zn(S,O,OH)/CdS	0.55	31.3	0.46	8.0	4.3	194.9

Figure 3. *J*–*V* curves of the CIGS solar cells fabricated with Ag NWs/CdS and Ag NWs + PEDOT:PSS/CdS and Ag NWs + PEDOT:PSS/Zn(S,O,OH)/CdS films.

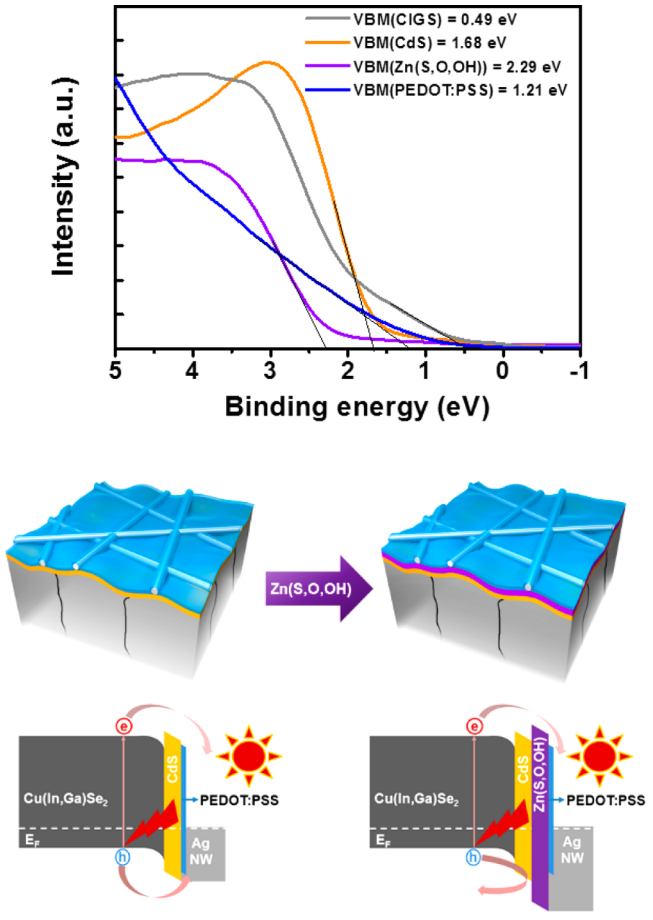

Figure 4. UPS spectra of CIGS, CdS, Zn(S,O,OH), and PEDOT:PSS films. The binding energy scale is referred to Fermi level.

The Ag NW network was deposited on the CdS/CIGS structure and evaluated for the cell efficiency. The CIGS solar cell used in this study has a clean and distinct CdS/CIGS interface, as shown in Figure 2a. Although the thin CdS layer has uniform coverage on top of the CIGS, a significantly high roughness can be observed because of the roughness of the CIGS layer. The electrostatically deposited Ag NWs were uniformly spread on the surface of the CdS film, and the

DOI: 10.1021/acsami.5b02989
ACS Appl. Mater. Interfaces 2015, 7, 13557–13563

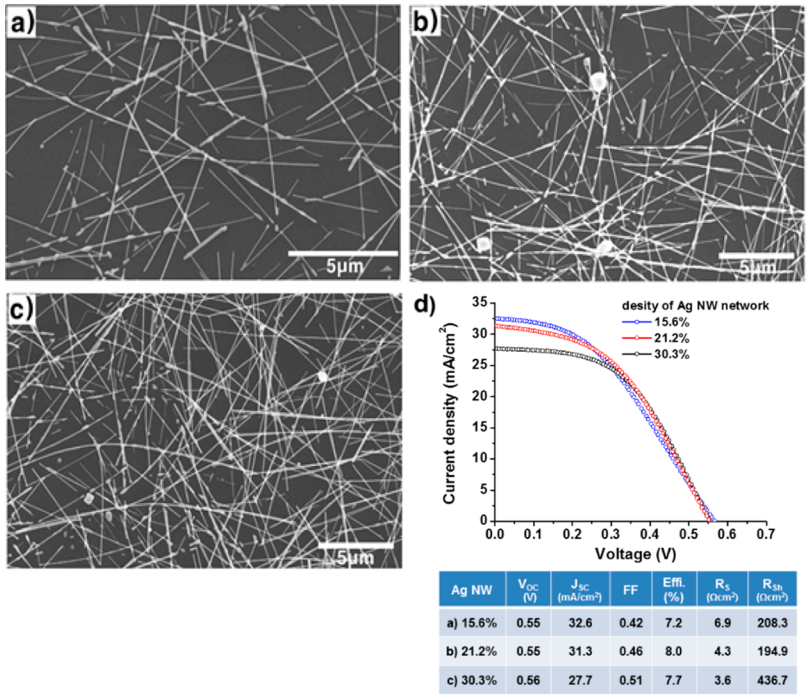

Ag NW	V_{OC} (V)	J_{SC} (mA/cm²)	FF	Effi. (%)	R_S (Ωcm²)	R_{Sh} (Ωcm²)
a) 15.6%	0.55	32.6	0.42	7.2	6.9	208.3
b) 21.2%	0.55	31.3	0.46	8.0	4.3	194.9
c) 30.3%	0.56	27.7	0.51	7.7	3.6	436.7

Figure 5. SEM images of the Ag NW network deposited using (a) 4 mL (areal density = 15.6%), (b) 7 mL (areal density = 21.2%), and (c) 10 mL (areal density = 30.3%) of the Ag NW dispersed solution. (d) $J-V$ curves of Ag NWs + PEDOT:PSS/Zn(S,O,OH)/CdS/CIGS solar cells with various densities of the Ag NW network.

separation distance among Ag NWs is approximately 1 μm, as shown in Figure 2b. The 10-nm-thick PEDOT:PSS as a conducting polymer was then coated on the Ag NW/CdS/CIGS sample, and the corresponding SEM image is shown in Figure 2c. PEDOT:PSS is expected to enhance the collection efficiency of the charge carriers that would otherwise have to travel across the CdS surface to reach the Ag NWs. Because the 10-nm-thick PEDOT:PSS surrounds the Ag NWs and bonds to the CdS surface, the adhesion of the Ag NW electrode is also expected to be enhanced.

The $J-V$ curves of the CIGS solar cells fabricated using the Ag NWs/CdS, Ag NWs + PEDOT:PSS/CdS, and Ag NWs + PEDOT:PSS/Zn(S,O,OH)/CdS films are shown in Figure 3. The CdS/CIGS solar cell with only the Ag NWs showed very poor performance. The shunt resistance (R_{sh}) of the Ag NWs/CdS/CIGS solar cell was 16.4 Ω cm^2 because of a high interfacial recombination at the interface. The short-circuit current (J_{sc}) was also small presumably because of insufficient contact between the long Ag NWs on a very rough surface of the CdS/CIGS layers. However, with the deposition of a 10-nm-thick PEDOT:PSS layer on the surface of the Ag NWs/CdS film, the J_{sc} value was significantly improved from 15.4 to 26.5 mA/cm^2. This is indicative of the role of PEDOT:PSS in a more effective collection of the charge carriers arriving at the CdS surface. Although J_{sc} was significantly increased with a thin PEDOT:PSS coating, V_{oc} of the cell was low, which indicated that the junction of the cell was still leaky.

The low V_{oc} can be understood by considering that the thickness of the CdS film is extremely thin, which is expected to be less effective in blocking the holes to flow toward the Ag NW/CdS interface for recombination. Additionally, the band gap of the CdS film is known to be 2.42 eV, which results in lowering the VBO at the CdS/CIGS interface. Generally, wide-band-gap materials can transmit light without absorption and also can increase the VBO at the interface. To lower the interfacial recombination, a Zn(S,O,OH) film (E_g > 3.3 eV) was introduced as a hole-blocking layer between the transparent electrode and CdS film. As a result of the Zn(S,O,OH) layer insertion, the efficiency of the CIGS solar cell was dramatically increased from 3.2 to 8.0%, where the V_{oc} value of the cell greatly increased from 0.35 to 0.55 V. Additionally, R_{sh} of the cell increased from 16.4 to 194.9 Ω cm^2. It is clear that insertion of the Zn(S,O,OH) film prevents the leakage current from interfacial recombination.

To verify that the increase in V_{oc} by adding the Zn(S,O,OH) film is arising from the VBO, the band alignment of the Zn(S,O,OH)/CdS/CIGS interface was studied using UPS analysis. The UPS spectra of CIGS, CdS, and Zn(S,O,OH) films are shown in Figure 4. The VBM values of the CIGS, CdS, and Zn(S,O,OH) films are 0.49, 1.68, and 2.29 eV, respectively, which leads to a VBO at the CdS/CIGS interface of 1.19 eV. By adding the Zn(S,O,OH) film on top of the CdS film, the VBO between the Zn(S,O,OH)and CIGS films was significantly increased from 1.19 to 1.8 eV. The increase of the VBO corresponds to a higher barrier to the transport hole at the interface. The solar cell with the Zn(S,O,OH) layer had sharply improved cell efficiency. Obviously, the Zn(S,O,OH) film could function as a hole-blocking layer to decrease interfacial recombination as a source of leakage current.

After ensuring improved charge collection efficiency with 10-nm-thick PEDOT:PSS and insertion of Zn(S,O,OH) as a hole-blocking layer, the density of the Ag NW network was revised to enhance J_{sc} further. J_{sc} of the solar cell is closely related to the degree of light transmittance. As expected, the transmittance of the film depends on the density of the Ag NW network, as shown in Figure 1. To optimize J_{sc} of the cell, the density of the Ag NW network was changed by adjusting the sprayed volume of the Ag NW dispersed solution. The SEM images of the Ag NW network with various densities are shown in Figure 5a–c. The densities of the Ag NW network deposited using 4, 7, and

DOI: 10.1021/acsami.5b02989
ACS Appl. Mater. Interfaces 2015, 7, 13557–13563

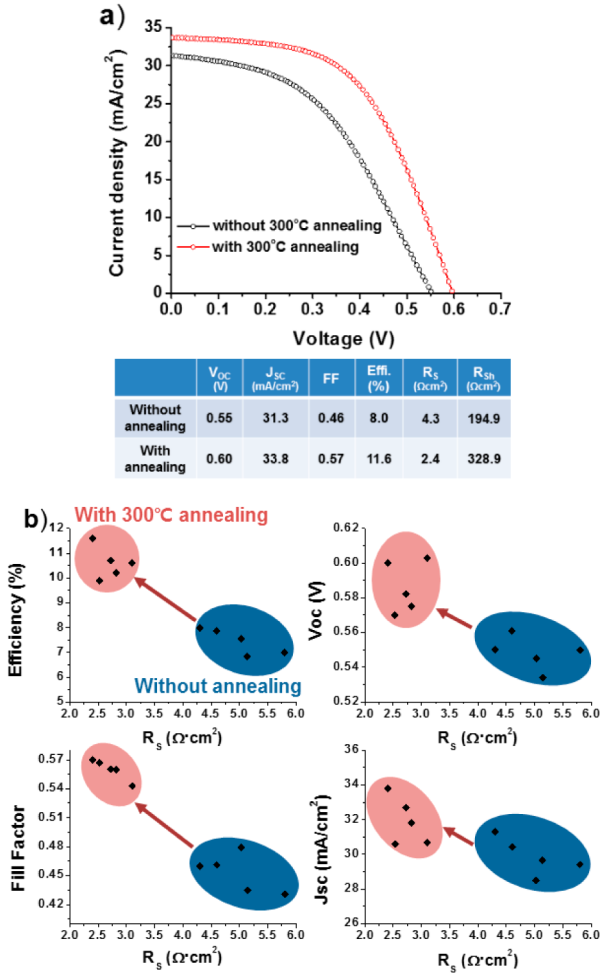

	V_{OC} (V)	J_{SC} (mA/cm²)	FF	Effi. (%)	R_S (Ωcm²)	R_{Sh} (Ωcm²)
Without annealing	0.55	31.3	0.46	8.0	4.3	194.9
With annealing	0.60	33.8	0.57	11.6	2.4	328.9

Figure 6. (a) $J-V$ curves. (b) R_s-resolved photovoltaic parameters of Ag NWs + PEDOT:PSS/Zn(S,O,OH)/CdS/CIGS solar cells with and without 300 °C heat treatment.

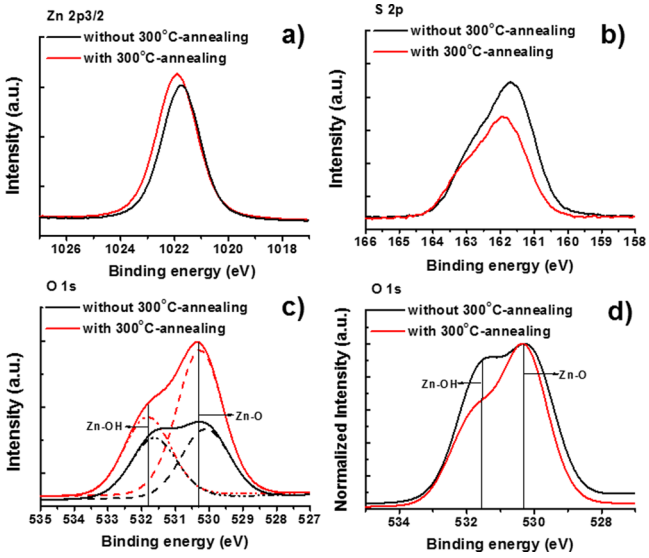

Figure 7. XPS spectra of (a) Zn $2p_{3/2}$, (b) S 2p, (c) O 1s, and (d) normalized O 1s for the Zn(S,O,OH) film before and after 300 °C heat treatment.

10 mL of the Ag NW dispersed solution were 15.6%, 21.2%, and 30.3%, respectively. As the density was increased, the Ag NW network was more compactly deposited, hence resulting in a decreased sheet resistance.

The $J-V$ curves of Ag NWs + PEDOT:PSS/Zn(S,O,OH)/CdS/CIGS solar cells with various densities of the Ag NW network are shown in Figure 5d. As the density of the Ag NW networks decreased, the J_{sc} value of the cell increased from 27.7 to 32.6 mA/cm^2 because of increased transmittance of the Ag NW network, but the fill factor (FF) of the cell decreased. In general, the FF value is affected by the resistance of the cell (series and shunt resistance), and thus the lowering of the FF value can be associated with an increase of the series resistance (R_s) of the cell. As shown in Figure 1b, the sheet resistance of the Ag NW network is shown to increase as the density of the Ag NWs decreases, which, in turn, can lower the FF. Therefore, it is important to tune the density of the Ag NW network to obtain maximum efficiency, where an optimum balance is needed between J_{sc} and R_s. Our results indicate that the optimal condition is to deposit the Ag NW network with a density of 21.2%. However, even with the optimized density of the Ag NWs, the $J-V$ curves showed that R_s is so large that it needs to be further reduced.

To decrease R_s in the cells without losing light transmittance, an additional heat treatment after deposition of the Zn(S,O,OH)/CdS film was conducted. The $J-V$ curves of Ag NWs + PEDOT:PSS/Zn(S,O,OH)/CdS/CIGS solar cells with and without 300 °C heat treatment of the Zn(S,O,OH)/CdS film are shown in Figure 6a. As a result of heat treatment, the cell efficiency significantly increased from 8.0 to 11.6%, where the R_s and FF values were greatly enhanced. In addition, R_s-resolved photovoltaic parameters for statistical analysis of the cell performance depending on the heat treatment are plotted in Figure 6b, which indicates that, after 300 °C heat treatment, the cell performance was highly enhanced because of a pronounced increase in FF, which could be responsible for the decrease in R_s of the solar cell. J_{sc} of the cell increased because of the reduction of R_s by an effective collection of electron carriers, and the increase in V_{oc} is determined to be due to a further increase in the VBM. According to UPS analysis, the VBM value of a 300 °C annealed Zn(S,O,OH) film increased slightly from 2.29 to 2.48 eV, hence resulting in effective hole blocking due to increased VBO. Heat treatment can result in a change in the chemical composition of the Zn(S,O,OH) film, which could be responsible for the increase in the VBO. This change in the VBO is consistent with other reports on the change in the electronic structure of the Zn(S,O,OH) film due to heat treatments under illumination.[25,26] A higher barrier at the interface due to an increase in the VBO can more effectively block the flow of hole carriers and reduce the interfacial recombination.

To understand the change in the valence-band structure of the Zn(S,O,OH) film, the film composition was studied by X-ray photoelectron spectroscopy (XPS). In general, the composition of a compound film is associated with the electronic band structure. The XPS spectra of Zn(S,O,OH) films on the CdS film before and after 300 °C heat treatment are shown in Figure 7. With 300 °C heat treatment, the binding energy and full-width at half-maximum values of the Zn element did not show a clear difference. However, the peak intensity of the S element decreased, which resulted from a loss in the volatile S element during 300 °C heat treatment. As shown in Figure 7c, O 1s XPS spectra can be deconvoluted as Zn−O and Zn−OH peaks.[27,28] The OH group content in the spectra of the O element also decreased from 0.9 to 0.65 after

DOI: 10.1021/acsami.5b02989
ACS Appl. Mater. Interfaces 2015, 7, 13557−13563

300 °C heat treatment. The bond of the OH groups with Zn ions is relatively weak so that it can be lost by a dehydration reaction. In the previous study, as the OH group content in the film decreases, the VBM of the film increases.[25,29] Thus, the composition change of the Zn(S,O,OH) film is associated with an increase of the VBO of the film. It improved V_{oc} by 300 °C heat treatment.

As explained previously, the solution-processed Ag NWs + PEDOT:PSS hybrid electrode that is fabricated using a low-cost, highly scalable method was shown to have excellent transparency and conductivity and can replace the transparent conducting oxide films that require high-cost vacuum processing. In order to maximize the efficiency of the CIGS solar cell with the Ag NWs + PEDOT:PSS hybrid electrode, the Zn(S,O,OH) hole-blocking layer that is heat-treated at 300 °C was used to reduce interfacial recombination. Our Ag NWs + PEDOT:PSS hybrid electrode that is optimized for the CIGS solar cell is expected to have advantages in having more mechanical flexibility in comparison to those containing vacuum-processed metal oxides and therefore opens up the possibility of developing more reliable flexible CIGS solar cells.

4. CONCLUSIONS

In this study, the Ag NWs + PEDOT:PSS hybrid electrode was developed as a low-cost, mechanically flexible alternative to the conducting oxide deposited by vacuum processes. The Ag NW network with transmittance and sheet resistance of above 85% and 17.5 Ω/sq, respectively, was determined to have the optimum areal density of the Ag NW network for optimized J_{sc} and V_{oc}. When a bare Ag NW network was deposited on the CdS film, the cell showed small J_{sc} due to insufficient contact between the long NWs and rough CdS surface. To increase J_{sc} of the cell, the PEDOT:PSS conducting polymer was used as a filler conducting polymer that can increase the collection efficiency of the charge carriers arriving at the CdS surface. As a result, J_{SC} significantly increased from 15.4 to 26.5 mA/cm^2. However, V_{oc} and R_{sh} were too low, which indicated that there was a significant amount of leakage current presumably due to interfacial recombination at the Ag NWs/CdS interface. To reduce the leakage current at the interface, a wide-band-gap Zn(S,O,OH) film was deposited between the CdS film and Ag NW network. The Zn(S,O,OH) film can provide a high barrier for blocking hole transport at the interface, and as a consequence V_{oc} was measured to have sharply improved from 0.35 to 0.55 V. In addition, the Zn(S,O,OH) film annealed at 300 °C was shown to have reduced OH groups and that induced a further increase in the VBO at the interface to reduce surface recombination further. Through optimization of the fabricating process, the best efficiency of 11.6% was achieved. Our study is the first report on an Ag NWs + PEDOT:PSS hybrid transparent electrode applied to CIGS solar cells with high efficiency.

AUTHOR INFORMATION

Corresponding Authors

*E-mail: btahn@kaist.ac.kr.
*E-mail: smhan01@kaist.ac.kr.

Author Contributions

‡Both authors equally contributed to this work.

Notes

The authors declare no competing financial interest.

ACKNOWLEDGMENTS

The authors thank the National Research Foundation of Korea for financial support under Contracts 2009-0094038 (Basic Science Research Program), 2012-0001167 and 2012-0001171 (Center for Inorganic Photovoltaic Materials), and 2014R1A4A1003712 (Basic Research Laboratory Program) as well as the Korea Research Council for Industrial Science & Technology under the contract number SC1100.

REFERENCES

(1) Goodrich, A.; Hacke, P.; Wang, Q.; Sopori, R. M.; James, T. L.; Woodhous, M. A Wafer-based Monocrystalline Silicon Photovoltaics Road Map: Utilizing Known Technology Improvement Opportunities for Further Reductions in Manufacturing Costs. *Sol. Energy Mater. Sol. Cells* **2014**, *114*, 110−135.

(2) Chirila, A.; Reinhard, P.; Pianezzi, F.; Bloesch, P.; Uhl, A. R.; Fella, C.; Kranz, L.; Keller, D.; Gretener, C.; Hagendorfer, H.; Jaeger, D.; Erni, R.; Nishiwaki, S.; Buecheler, S.; Tiwari, A. N. Potassium-induced Surface Modification of $Cu(In,Ga)Se_2$ Thin Films for High-efficiency Solar Cells. *Nat. Mater.* **2013**, *12*, 1107−1111.

(3) Jackson, P.; Hariskos, D.; Lotter, E.; Paetel, S.; Wuerz, R.; Menner, R.; Wischmann, W.; Powalla, M. New World Record Efficiency of $Cu(In,Ga)Se_2$ Thin Films Solar Cells Beyond 20%. *Prog. Photovoltaics* **2011**, *19*, 894−897.

(4) Hibberd, C. J.; Chassaing, E.; Liu, W.; Mitizi, D. B.; Licot, D.; Tiwari, A. N. Non-vacuum Methods for Formation of $Cu(In,Ga)(Se,S)_2$ Thin Film Photovoltaic Absorbers. *Prog. Photovoltaics* **2012**, *18*, 434−452.

(5) Todorov, T. K.; Gunawan, O.; Gokmen, T.; Mitzi, D. B. Solution-processed $Cu(In,Ga)(S,Se)_2$ Absorber Yielding a 15.2% Efficient Solar Cell. *Prog. Photovoltaics* **2013**, *21*, 82−87.

(6) Bag, S.; Gunawan, O.; Gokmen, T.; Zhu, Y.; Todorov, T. K.; Mitzi, D. B. Low Band Gap Liquid Processed CZTSe Solar Cell with 10.1% Efficiency. *Energy Environ. Sci.* **2012**, *5*, 7060−7065.

(7) Shin, B.; Gunawan, O.; Zhu, Y.; Bojarczuk, N. A.; Chey, S. J.; Guha, S. Thin Film Solar Cell with 8.4% Power Conversion Efficiency Using an Earth-abundant Cu_2ZnSnS_4 Absorber. *Prog. Photovoltaics* **2013**, *21*, 72−76.

(8) Walsh, A.; Chen, S.; Wei, S.; Gong, X. Kesterite Thin Film Solar Cells: Advances in Materials Modelling of Cu_2ZnSnS_4. *Adv. Energy Mater.* **2012**, *2*, 400−409.

(9) Yin, X.; Tang, C.; Sun, L.; Shen, Z.; Gong, H. Study on Phase Formation Mechanism of Non- and Near-Stoichiometric $Cu_2ZnSn(S,Se)_4$ Film Prepared by Selenization of Cu−Sn−Zn−S Precursors. *Chem. Mater.* **2014**, *26*, 2005−2014.

(10) Nam, S.; Song, M.; Kim, D.; Cho, B.; Lee, H.; Kwon, J.; Park, S.; Nam, K.; Jeong, Y.; Kwon, S.; Park, Y.; Jin, S.; Kang, J.; Jo, S.; Kim, C. Ultrasmooth, Extremely Deformable and Shape Recoverable Ag nanowire Embedded Transparent Electrode. *Sci. Rep.* **2014**, *4*, 1−7.

(11) Lee, H.; Hwang, J.; Choi, K.; Jung, S.; Kim, K.; Shim, Y.; Park, C.; Park, Y.; Ju, B. Effective Indium-doped Zinc Oxide Buffer Layer on Silver Nanowires for Electrically Highly Stable, Flexible, Transparent, and Conductive Composite Electrodes. *ACS Appl. Mater. Interfaces* **2013**, *5*, 10397−10403.

(12) Langley, D.; Giusti, G.; Lagrange, M.; Collins, R.; Jimenez, C.; Brechet, Y.; Bellet, D. Silver Nanowire Networks: Physical Properties and Potential Integration in Solar Cells. *Sol. Energy Mater. Sol. Cells* **2014**, *125*, 318−324.

(13) Krantz, J.; Stubhan, T.; Richter, M.; Spallek, S.; Litzov, I.; Matt, G. J.; Spiecker, E.; Brabec, C. J. Sprayed-coated Silver Nanowires as Top Electrode Layer in Semitransparent P3HT:PCBM-based Organic Solar Cells Devices. *Adv. Funct. Mater.* **2013**, *23*, 1711−1717.

(14) Song, M.; You, D.; Lim, K.; Park, S.; Jung, S.; Kim, C.; Kim, D.; Kim, D.; Kim, J.; Park, J.; Kang, Y.; Heo, J.; Jin, S.; Park, J.; Kang, J. Highly Efficient and Bendable Organic Solar Cells with Solution-processed Silver Nanowire Electrodes. *Adv. Funct. Mater.* **2013**, *23*, 4177−4184.

DOI: 10.1021/acsami.5b02989
ACS Appl. Mater. Interfaces 2015, 7, 13557−13563

(15) Chung, C.; Song, T.; Bob, B.; Zhu, R.; Duan, H.; Yang, Y. Silver Nanowire Composite Widow Layers for Fully Solution-deposited Thin Film Photovoltaics Devices. *Adv. Mater.* **2012**, *24*, 5499−5504.
(16) Kim, A.; Won, Y.; Woo, K.; Jeong, S.; Moon, J. All-solution-processed Indium-free Transparent Composite Electrodes Based on Ag Nanowire and Metal Oxide for Thin-film Solar Cells. *Adv. Funct. Mater.* **2014**, *24*, 2462−2471.
(17) Xu, Q.; Song, T.; Chi, W.; Liu, Y.; Xu, W.; Lee, S.-T.; Sun, B. Solution-processed Highly Conductive PEDOT:PSS/AgNW/GO Transparent Film for Efficient Organic−Si Hybrid Solar Cells. *ACS Appl. Mater. Interfaces* **2015**, *7*, 3272−3279.
(18) Sun, Y.; Yin, Y.; Mayers, B. T.; Herricks, T.; Xia, Y. Uniform Silver Nanowires Synthesis by Reducing $AgNO_3$ with Ethylene Glycol in the Presence of Seeds and Poly(vinyl pyrrolidone). *Chem. Mater.* **2002**, *14*, 4736−4745.
(19) Lee, J.; Conner, S. T.; Cui, Y.; Peumans, P. Solution-processed Metal Nanowire Mesh Transparent Eectrodes. *Nano Lett.* **2008**, *8*, 689−692.
(20) Kim, T.; Canlier, A.; Kim, G.; Choi, J.; Park, M.; Han, S. Electrostatic Spray Deposition of Highly Transparent Silver Nanowire Electrode on Flexible Substrate. *ACS Appl. Mater. Interfaces* **2013**, *5*, 788−794.
(21) Kim, K.; Yoon, K.; Yun, J.; Ahn, B. Effects of Se Flux on the Microstructure of $Cu(In,Ga)Se_2$ Thin Film Deposited by a Three-stage Co-evaporation Process. *Electrochem. Solid-State Lett.* **2006**, *9*, A382−A385.
(22) Shin, D.; Shin, Y.; Kim, J.; Ahn, B.; Yoon, K. Control of the Preferred Orientation of $Cu(In,Ga)Se_2$ Thin Film by the Surface Modification of Mo Film. *J. Electrochem. Soc.* **2012**, *159*, B1−B5.
(23) Shin, D.; Larina, L.; Yoon, K.; Ahn, B. Fabrication of $Cu(In,Ga)Se_2$ Solar Cell with ZnS/CdS Double Layer as an Alternative Buffer. *Curr. Appl. Phys.* **2010**, *10*, S142−S145.
(24) Larina, L.; Shin, D.; Kim, J.; Ahn, B. Alignment of Energy Levels at the ZnS/$Cu(In,Ga)Se_2$ Interface. *Energy Environ. Sci.* **2011**, *4*, 3487−3493.
(25) Shin, D.; Kim, S.; Kim, J.; Kang, H.; Ahn, B.; Kwon, H. Study of Band Btructure at the Zn(S,O,OH)/$Cu(In,Ga)Se_2$ Interface via Rapid Thermal Annealing and Their Effect on the Photovoltaic Properties. *ACS Appl. Mater. Interfaces* **2013**, *5*, 12921−129277.
(26) Kobayashi, T.; Yamaguchi, H.; Nakada, T. Effects of Combined Heat and Light Soaking on Device Performance of $Cu(In,Ga)Se_2$ Solar Cells with ZnS(O,OH) Buffer layer. *Prog. Photovoltaics* **2014**, *22*, 115−121.
(27) Nakada, T.; Furumi, K.; Kunioka, A. High-efficiency Cadmium-free $Cu(In,Ga)Se_2$ Thin-film Solar Cells with Chemically Deposited ZnS Buffer Layers. *IEEE Trans. Electron Devices* **1999**, *46*, 2093−2097.
(28) Shin, D.; Kim, J.; Kim, S.; Larina, L.; Al-Ammar, E. A.; Ahn, B. Growth of a High-quality Zn(S,O,OH) Thin Film via Chemical Bath Deposition for Cd-free $Cu(In,Ga)Se_2$ Solar Cells. *Sol. Energy Mater. Sol. Cells* **2013**, *116*, 76−82.
(29) Nakada, T.; Kobayashi, T.; Kumazawa, T.; Yamaguchi, H. Impacts of Post-treatments on Cell Performance of CIGS Solar Cells with Zn Compound Buffer Layers. *IEEE J. Photovolt.* **2013**, *3*, 461−466.

DOI: 10.1021/acsami.5b02989
ACS Appl. Mater. Interfaces 2015, 7, 13557−13563